The FASEB Journal express article 10.1096/fj.00-0645fje. Published online May 9, 2001.

Protein and peptide delivery via engineered polyomavirus-like particles

Constanze Günther,*[,†,1] Uli Schmidt, *[,†,1] Rainer Rudolph,* and Gerald Böhm[†]

*Institut für Biotechnologie, Martin-Luther-Universität Halle-Wittenberg, 06120 Halle (Saale), Germany; [†]ACGT ProGenomics AG, 06120 Halle (Saale), Germany. [1]These authors contributed equally to the following work.

Corresponding author: Constanze Günther, Institut für Biotechnologie, Martin-Luther-Universität Halle-Wittenberg, Kurt-Mothes-Str. 3, 06120 Halle (Saale), Germany. E-mail: constanze.guenther@biochemtech.uni-halle.de

ABSTRACT

Recent advances in molecular biology have led to the development of new therapeutics to address genetic disorders. The developments in the production and availability of recombinant proteins are likely to have a substantial impact on many diseases in the short term. A major limit for the use of recombinant proteins in clinical applications is their inability to enter cells and be targeted to the appropriate intracellular site. Here, we describe a novel system for the intracellular delivery of peptides and proteins using recombinantly expressed polyomavirus-like particles as universal carriers. The inner surface of the particles was modified by the fusion of a WW domain, which was derived from the mouse formin binding protein 11 (FBP11) to the viral coat protein in order to bind specifically to proline-rich ligands. Physicochemical characterization of the fusion protein demonstrated that the functional units of the VP1-WW protein remained intact. Assembly of the particles in the presence of proline-rich ligands resulted in an efficient encapsidation of the ligands into the particles. Fluorescence-labeled peptides and the green fluorescent protein were used as model ligands. The delivery of the ligands into cultured eukaryotic cells could be demonstrated with confocal laser-scanning microscopy.

Key words: drug delivery • in vitro assembly • VP1 • WW domain

With an increasing understanding of the pathogenesis of many diseases on a molecular level it is now possible to use recombinant proteins for the functional substitution of defective or missing proteins, or for the modulation of metabolic or signal transduction pathways (1). However, most proteins are unable to enter cells and to reach intracellular targets and are therefore limited to extracellular application. Recently, fusions of target proteins with viral protein sequences of either HIV TAT (2) or herpes simplex virus VP22 (3) were found to mediate transfer of the target protein across the plasma membrane into cells. Here, we describe a novel system for the transduction of proteins, peptides, and other compounds based on specifically modified polyomavirus-like particles that can efficiently encapsidate the compounds for the delivery into target cells.

The icosahedral shell of murine polyomavirus is composed of 72 pentameric subunits of the major capsid protein VP1 and an inner layer of the minor capsid proteins VP2 and VP3. The outer capsid protein VP1 can be expressed and purified from recombinant *Escherichia coli* (4-6) and spontaneously forms virus-like particles in vitro in the presence of Ca^{2+} ions without the need of VP2 or VP3 (7, 8). The crystal structures of the capsid and of proteolytically truncated pentameric VP1 have been reported (9-11). The C-terminal end of VP1 interacts with neighboring pentamers and mediates the contacts within the viral capsid (9). The flexible N-terminal end is supposed to interact with the viral DNA genome (12) and is located at the inner surface of the capsid (9, 11).

Because polyomavirus-like particles are well characterized and can easily be produced in large quantities, VP1 gained attention for the in vitro packaging of plasmid DNA in order to develop a nonviral gene therapy vector that exploits viral mechanisms for gene transfer (13, 14). However, the in vitro packaging of plasmid DNA is still inefficient, and transfection efficiencies are low compared with those of viral vectors. A different approach is the packaging of oligonucleotides into polyomavirus-like particles, which is reported to be significantly more effective (15), but successful transport of the packaged compounds into eukaryotic cells has so far not been demonstrated.

MATERIALS AND METHODS

Protein modelling

Structures of VP1-WW and green fluorescent protein (GFP)-PPLP were modeled by using the program Modeller 4 (16) based on the published structures of VP1 at a resolution of 1.9 Å and 3.65 Å, respectively (10, 11), and of wild-type GFP (17). The FBP11 WWa domain was modeled by using the published NMR structure of the YAP WW domain (18). Figures were generated by MolScript (19) and Raster3D (20).

Cloning and vector construction

The FBP11 WWa domain was amplified by polymerase chain reaction (PCR) by using the oligonucleotides WW-5' (5'-TAT TAA TCA TAT GAG CGG CTG GAC AGA ACA TAA ATC ACC TGA TGG-3') and WW-3' (5'-AAT ATA TCA TAT GTC CAT CAT CCG GCT TTT CCC AGG TAG ACT G-3'). The resulting PCR product was cloned via introduced *Nde*I restriction sites into the plasmid pET21-VP1-3C-Int, which contained the VP1 gene with a minimal pattern of cysteine

residues necessary for in vitro assembly and site-specific fluorescence labeling (5, 21), and a C-terminal fusion with an intein and a chitin binding domain for affinity chromatography.

The GFP gene was amplified via PCR by using the oligonucleotides GFP-NdeI-5' (5'-TTA TTT ACA TAT GGT GAG CAA GGG CGA GGA G-3') and GFP-AflII-3' (5'-ATA TCT TAA GTA CAG CTC GTC CAT GCC G-3') and was cloned into the plasmid pTIP, which contained a T7lac promoter for high-level expression in *E. coli*, as well as the sequence of the C-terminal PPLP tag and intein/chitin binding domains for affinity chromatography.

Protein expression and purification

All proteins were expressed from recombinant *E. coli* and purified as described before (5), except that in the case of GFP-PPLP the growth temperature of the cultures was kept at 37°C after induction with isopropyl-ß-D-thiogalactopyranoside.

In vitro assembly, size-exclusion chromatography, and determination of encapsidation efficiencies

Particles were assembled in vitro according to Salunke et al. (7, 8). For the encapsidation into virus-like particles, the proline-rich ligands were added at an up to fivefold molar excess before the assembly process was started. The capsid assembly process was quantitatively analyzed by high-pressure liquid chromatography (HPLC) size-exclusion chromatography with columns of 14 ml of TSKgel 5000PW_{XL} or 6000PW_{XL} (Toso Haas, Stuttgart, Germany), as described earlier (5). The absorptions of the proteins at 280 nm and of the chromophores at 490 or 583 nm, respectively, were recorded simultaneously. After integration of the peak areas, the in vitro assembly efficiencies and the encapsidation rates were calculated from the number of molecules within the fractionated peaks by using the following equation:

$$n = \frac{A \cdot F \cdot f}{\varepsilon \cdot d}$$

with n = number of molecules; A = peak area (µAU); F = flow rate (usually 0.7 ml/min); f = unit correction factor ($1/6 \cdot 10^{-10}$); ε = molar extinction coefficient (cm^{-1} M^{-1}); and d = light path in the flow cell of the HPLC detector (0.06 mm). Then, the number of GFP or peptide molecules (measured at 490 or 583 nm, respectively) was set in relation to the number of capsid molecules (detected at 280 nm), which was calculated by the equation given above. The absorption of GFP at 280 nm in the capsid peak (calculated from the respective data at 490 nm) was substracted from the total absorption prior to the calculation of VP1 capsids in the fraction, in order to correct for the GFP contribution to A_{280}.

Surface plasmon resonance

In order to determine the affinity of the VP1-WW fusion protein to polyproline sequences, surface plasmon resonance was measured with a Biacore X (Biacore AB, Freiburg, Germany) and a CM5 sensorchip that was coated with PPLP peptide (sequence: $CSGP_6PPLP$), following the manufacturer's protocol. The protein concentrations were varied between 5 and 50 nM. Kinetic parameters were calculated with the BIAevaluation software using a simple Langmuir binding model.

Circular dichroism (CD) spectroscopy

Far-UV CD spectra, from 195 to 260 nm, of VP1 variants were measured in 0.1-mm cuvettes. The proteins (0.4-0.5 mg/ml) were dialyzed against a buffer containing 10 mM HEPES and 100 mM NaCl, pH 7.2. Spectra of the buffer were also recorded and subtracted from the protein spectra to eliminate noise contributions from the buffer. The secondary structure content of the proteins was calculated with the program CDNN (22) from the buffer-corrected spectra.

Electron microscopy

An EM 912 instrument (Zeiss) was used for electron microscopy studies, with application of a magnification factor of 63,000. The specimen was stained with uranyl acetate on bacitracin-incubated (0.1 mg/ml, 1 min) copper-carbon grids according to standard protocols.

Delivery experiments

Cultures of C2C12 myoblasts or NIH 3T3 fibroblasts were grown in 8-well chambered cover glasses (Nunc, Wiesbaden, Germany). The cultures were incubated from 15 min up to 2 h with 0.5-1.0 nM fluorescence-labeled virus-like particles encapsidating GFP or fluorescence-labeled peptides. In addition, in some samples lysosomes were stained with 1 µM LysoSensor yellow/blue (Molecular Probes, Göttingen, Germany). After incubation, cells were washed two times with PBS and covered with noncolored Dulbecco's modified Eagle medium. Cells were subsequently analyzed with a LSM410 confocal laser-scanning microscope equipped with a 63-fold water immersion objective (Zeiss).

RESULTS

Principle of directed encapsidation

To encapsidate peptides and proteins into polyomavirus-like particles, modifications of the inner capsid surface were generated to achieve a specific interaction of the free capsomeres with peptides or proteins that are directed into the capsids upon induction of in vitro assembly (**Fig. 1*a***). The first WW domain of the mouse formin binding protein 11 (FBP11) was fused to the N terminus of VP1 as a module to facilitate this interaction. WW domains are small protein domains and were first discovered in the Yes kinase-associated protein (YAP) of *Saccharomyces cerevisiae* (23, 24). They were named after two conserved tryptophan residues, which are essential for the maintenance of the native fold and for ligand binding (25). The FBP11 WW domains bind proline-rich ligands with the consensus motif PPLP (26).

Protein modeling studies of the VP1-WW fusion protein (**Fig. 1*b***) revealed that there is sufficient space inside the capsid to allow proper folding and arrangement of the WW domains. Given that there are 360 ligand binding sites (72 pentameric VP1 molecules per capsid) inside each capsid, it was calculated that

theoretically 360 globular proteins with an average size of up to 17 kDa can be encapsidated. In the case of lower encapsidation rates, for example, using only two of the five potential binding sites per pentamer, a capsid could accomodate 144 molecules of a 90-kDa protein.

Recombinant VP1-WW obtained a native fold and bound proline-rich ligands

The fusion protein VP1-WW, solubly expressed and purified from recombinant *E. coli*, was characterized with respect to correct protein folding and ligand binding of the WW domain. To confirm the native fold, far-UV CD spectra of the VP1-WW fusion protein were recorded and compared with the spectrum of the wild-type protein (**Fig. 2**). As expected, the VP1-WW spectrum had a significantly increased negative ellipticity difference ($\Delta\varepsilon$) below 207 nm, indicating a higher portion of β-sheet secondary structure than in wild-type VP1. The difference spectrum of VP1-WW minus VP1 should represent the spectrum of the single WW domain. This difference CD spectrum of VP1-WW had a maximum at 230 nm and an intense negative ellipticity at <205 nm (**Fig. 2*b***). The difference spectrum corresponds closely to a typical WW domain spectrum that was published earlier (27), indicating that the WW domain obtains its native fold in the context of the fusion protein VP1-WW.

The integrity and functionality of the fused WW domain were further verified by surface plasmon resonance by using an immobilized PPLP peptide ligand. Samples of the fusion protein were measured at different concentrations, and association and dissociation reactions were recorded (**Fig. 3**). The dissociation seems to be a two-phase reaction, starting with an initial fast step, which may be due to an unspecific hydrophobic interaction, and the subsequently following slow dissociation as a result of the specific interaction between the WW domain and the PPLP peptide. Another explanation would be that some of the VP1-WW pentamers interact with the ligand through only one WW monomer and are therefore prone to fast dissociation (first phase). The simultaneous binding of the pentameric VP1-WW protein with more than one WW domain to the sensor surface results in a considerably slower dissociation rate (second phase). However, the latter explanation is contradicted by measurements with a monomeric protein containing a WW domain (28), which shows a similar two-step dissociation curve. Within the time frame of the Biacore experiment, the baseline was not reached again, i.e., the complete dissociation of the VP1-WW from the sensor surface was not observed.

Determination of the kinetic parameters yielded an equilibrium dissociation constant $K_d = 40 \pm 5$ nM. This result is in good agreement with former surface plasmon resonance data using a fusion protein of glutathione *S*-transferase and the FBP11 WW domain (28); the K_d for this protein was reported to be 21 nM. The interaction of the WW domain with its ligand is highly specific, because measurements in the presence of other proteins did not inhibit binding to the sensorchip surface, whereas the free PPLP peptide was a potent inhibitor of the association (data not shown). These observed features, i.e., correct protein fold and specific binding of PPLP ligands, are important prerequisites for an encapsidation of PPLP-tagged peptides and recombinant proteins.

VP1-WW encapsidated proline-rich ligands

Either PPLP-tagged GFP or fluorescence-labeled PPLP peptides were used as model ligands for optimization of the encapsidation. In the latter case, the fluorescent dye also represented a model for the delivery of small chemical compounds linked to a PPLP-containing peptide.

Encapsidation rates were determined by size-exclusion chromatography, which separates virus-like particles from free capsomeres and the engaged ligands, PPLP peptide (**Fig. 4*a***) or GFP (**Fig. 4*c***) (5). The specific absorbance or fluorescence in the elution fraction of the capsid clearly showed that the ligands coeluted with the capsid. The maximum encapsidation rate, subject to optimal assembly conditions, was 230 peptide molecules and 260 GFP molecules per virus-like particle. The encapsidation increased with an increasing ligand/capsomere ratio and reached a maximum at a fivefold excess of ligand to capsomeres (data not shown). A further increase of the ligand concentration resulted in a decrease in the efficiency of in vitro assembly instead of higher encapsidation rates (data not shown). This effect might be due to steric interferences of the GFP, especially because theoretical calculations of the packing density inside the particles also suggested a spatial limit of approximately 280 GFP molecules per capsid. In addition, higher concentrations of the PPLP sequence or the fluorescent dye may nonspecifically inhibit protein-protein interactions required for capsid formation.

Size-exclusion chromatography was further used for the preparative separation of virus-like particles, capsomeres, and free ligands to ensure preparations of the highest purity and homogeneity for subsequent experiments. To further confirm the data from size-exclusion chromatography, the morphology and integrity of the isolated virus-like particles were verified by electron microscopy (**Fig. 4*b*** and ***d***). The size and morphology of the capsids were indistinguishable from those of empty wild-type particles, thus providing further evidence that the ligands were successfully embedded in these virus-like particles.

Protein and peptide delivery into cultured cells

The ability of polyomavirus-like particles to transfer encapsidated molecules into eukaryotic cells was examined in tissue cultures in vitro. Virus-like particles containing either fluorescence-labeled peptides or GFP were isolated by using size-exclusion chromatography, as described above. Cultures of NIH 3T3 mouse fibroblasts were incubated with the particles and analyzed by confocal laser scanning microscopy. Significant fluorescence was detected within all cells even after a 30-min incubation (**Fig. 5**). The fluorescent molecules were localized near the cell membrane (**Fig. 5*a***) and eventually (after 2 h of incubation) showed greater distribution throughout the entire cytoplasm, indicating that encapsidated ligands were rapidly and efficiently delivered. There was no observable difference between encapsidated peptides and GFP with respect to delivery efficiency and subcellular distribution.

To determine the distribution of capsids and encapsidated ligands individually, the capsid protein VP1 was labeled with a different fluorescent dye at a specific cysteine residue (21) in addition to the fluorescent ligands. Therefore, in uptake

experiments into NIH 3T3 cells the capsid proteins and the ligands could be detected simultaneously and distinguished by their fluorescence properties. Within the time frame of the experiments, most of the ligands were still colocalized with the capsid proteins (**Fig. 5**), which may be attributed to the tight binding between the WW domain and its ligand. However, there was also noncolocalized fluorescence of capsid proteins as well as of ligands, indicating that at least partial release of the ligands from the capsids occurred. The mechanism of dissociation of the ligands from the VP1 transport vehicles inside the cells is still unknown; either dissociation occurs faster under in vivo conditions than in our in vitro experiments, or at least partial degradation of the carrier and/or the ligand protein occurred. Because GFP fluorescence (which is based on an intact GFP protein structure) could be found in the cytosol of the cells, complete degradation of carrier and ligand is unlikely. Although capsids and ligands were also found together in endocytotic vesicles, the simultaneous staining of lysosomes revealed only weak colocalization with the peptides (**Fig. 5*e*** and ***f***). Therefore, a release of most ligands into the cytoplasm of the cells seems possible.

DISCUSSION

The major capsid protein VP1 of murine polyomavirus was engineered for a directed encapsidation of peptides and proteins tagged with a proline-rich sequence. The WW domain was found to be very useful because it is the smallest protein domain known so far (29) and provides specific noncovalent binding with an affinity sufficient to link ligands to the capsomeres during the in vitro assembly process of the virus-like particles. The fusion to the viral capsid protein VP1 did not substantially change the properties of the WW domain with respect to ligand binding. Also, VP1 remained its native structure and maintained the ability to form virus-like particles in vitro, similar to the wild-type protein. It was possible to encapsidate a maximum of 230 peptide molecules and 260 molecules of the model protein GFP per capsid. This is significantly more than the statistically expected inclusion of less than three molecules, considering the capsid and ligand concentrations used here, although the theoretical limit of encapsidation is not yet reached, probably because of the fast association/dissociation equilibrium between the proline-rich ligands and the WW domain. The directed encapsidation presented here has substantial advantages over liposome-based peptide and protein delivery, because all steps are carried out under mild conditions in buffered aqueous solutions. In addition, because of the specific interactions of the capsomeres with the ligands, comparatively low ligand concentrations can be used, thus avoiding aggregation of the ligands at high concentrations.

The drug delivery system presented here is generally applicable to the delivery of a wide range of peptides, small PPLP-tagged compounds, and proteins. It must be ensured that the PPLP tag that is necessary for encapsidation does not interfere with the biological function of the compounds. In most cases this should not be limiting, because the PPLP motif is highly water soluble, and a careful selection of the incorporation site of the sequence or the design of linker molecules should circumvent structural and sterical interferences with the activity of the therapeutic substances. Possible limitations for the encapsidation of proteins may arise for large proteins. A maximum encapsidation of 260 molecules per capsid was found for the 27-kDa protein GFP, which is in good agreement with theoretical calculations. However, many useful proteins may be substantially larger than 27 kDa and may decrease the in vitro assembly of the capsids because of steric hindrance. This effect might be avoided by using mixed capsids. It was demonstrated that capsids can be assembled in vitro from differently modified capsomeres in a mosaic-like fashion (own unpublished results). With this strategy, the number of ligand binding sites within the capsids could be adjusted by mixing VP1-WW capsomeres with wild-type capsomeres for an optimized encapsidation and in vitro assembly efficiency. Other limitations may arise for homo-oligomeric proteins carrying several PPLP tags. Although we did not examine such proteins yet, it is likely that multiple binding sites lead to an increased aggregation of the capsomeres and the ligand protein.

Cell culture experiments demonstrated an efficient uptake of the vector and the delivery of the encapsidated substances. Only a small fraction of the ligands in cellular lysosomes is targeted for degradation. There is an approximately equal distribution of the ligands within the cytoplasm and ligands still remaining in endosomes. There is not much known about endosomal release of polyomavirus-like particles, and therefore these observations cannot yet be fully explained. For the native virus, myristylation of the minor coat protein VP2 may have a crucial function for endosomal release (30), and empty polyomavirus-like particles consisiting of only VP1 are mostly targeted to lysosomes (own unpublished results). However, virus-like particles and the native virus may use different routes of entry into the cells, and mechanisms utilized by the wild-type virus may not be effective for virus-like particles. In future studies, mechanisms for the improvement of endosomal escape, for example, coupling of fusogenic peptides, will be evaluated for the further improvement of drug delivery.

Compared with the use of fusion proteins with viral sequences (2, 3), encapsidation into virus-like particles has the advantage that the ligands are protected inside a protein shell from external proteases and from recognition by the immune system, although the particles themselves may be immunogenic. However, the particles can be modified, for example, via specific cysteine residues, with polymers such as polyethylene glycol, which is known to suppress the host immune response (31), without the need to modify the therapeutic peptide or protein itself. The strategy of mixed capsid assembly may also be exploited to combine different functions within the vector. For example, capsomeres that facilitate encapsidation of the ligands could be combined with capsomeres modified on the outer surface in order to target only specific cell types. This feature holds great potential for the improvement of new and existing drugs, e.g., the delivery of cytostatic drugs only into tumor tissue would drastically reduce side effects. It is also conceivable to fuse other WW domains to the VP1 capsomeres, which recognize different proline-rich sequences. During in vitro assembly with various VP1-WW fusion capsomeres, different ligands could be encapsidated and administered simultaneously with an exactly defined ratio. For example, emerging resistance of tumor cells to a single drug could be prevented by applying a mixture of diverse drugs.

In summary, it is envisaged that engineered virus-like particles as modular delivery systems could greatly enhance the use of therapeutic peptides and recombinant proteins. Such multifunctional drug delivery systems may be useful for the treatment of human diseases in the future.

ACKNOWLEDGMENTS

We thank Dr. Mark Bedford, Harvard Medical School, Boston, MA, for providing the plasmid containing the gene of the FBP11 WW domain; Dr. Dieter Neumann, Institut für Pflanzenbiochemie, Halle, Germany, for his help with electron microscopy; and Dr. Bettina Hause, Institut für Pflanzenbiochemie, Halle, Germany, for assistance with confocal laser-scanning microscopy. We also acknowledge Ms. Doreen Siegemund from our laboratory for excellent technical assistance. This work was supported by a grant from Land Sachsen-Anhalt.

REFERENCES

1. Russel, C.S. & Clarke, L.A. (1999) Recombinant proteins for genetic disease. *Clin. Genet*. **55,** 389-394
2. Schwarze, S.R., Ho, A., Vocero-Akbani, A. & Dowdy, S.F. (1999) In vivo protein transduction: delivery of a biologically active protein into the mouse. *Science* **285,** 1569-1572
3. Elliot, G. & O'Hare, P. (1997) Intercellular trafficking and protein delivery by a herpesvirus structural protein. *Cell* **88,** 223-233
4. Leavitt, A.D., Roberts, T.M. & Garcea, R.L. (1985) Polyomavirus major capsid protein VP1: purification after high level expression in *Escherichia coli*. *J. Biol. Chem*. **23,** 12803-12809
5. Schmidt, U., Rudolph, R. & Böhm, G. (2000) Mechanism of assembly of recombinant polyomavirus-like particles. *J. Virol*. **74,** 1658-1662
6. Stubenrauch, K., Bachman, A., Rudolph, R. & Lilie, H. (2000) Purification of a viral coat protein by an engineered polyionic sequence. *J. Chromatogr. B Biomed. Appl*. **737,** 77-84
7. Salunke, D.M., Caspar, D.L. & Garcea, R.L. (1986) Self-assembly of purified polyomavirus capsid protein VP1. *Cell* **46,** 895-904
8. Salunke, D.M., Caspar, D.L. & Garcea, R.L. (1989) Polymorphism in the assembly of polyomavirus capsid protein VP1. *Biophys. J*. **56,** 887-900
9. Stehle, T., Yan, Y., Benjamin, T.L. & Harrison, S.C. (1994) Structure of murine polyomavirus complexed with an oligosaccharide receptor fragment. *Nature (London)* **369,** 160-163
10. Stehle, T. & Harrison, S.C. (1996) Crystal structures of murine polyomavirus in complex with straight-chain and branched-chain sialyloligosaccharide receptor fragments. *Structure* **4,** 183-194
11. Stehle, T. & Harrison, S.C. (1997) High-resolution structure of a polyomavirus VP1-oligosaccharide complex: implications for assembly and receptor binding. *EMBO J*. **16,** 5139-5148
12. Chang, D., Cai, X. & Consigli, R.A. (1993) Characterization of the DNA binding properties of polyomavirions capsid proteins. *J. Virol*. **67,** 6327-6331
13. Forstova, J., Krauzewicz, N., Sandig, V., Elliot, J., Palkova, Z., Strauss, M. & Griffin, B.E. (1995) Polyomavirus pseudocapsids as efficient carriers of heterologous DNA into mammalian cells. *Hum. Gene Ther*. **6,** 297-306
14. Soeda, E., Krauzewicz, N., Cox, C., Stokrova, J., Forstova, J. & Griffin, B.E. (1998) Enhancement by polylysine of transient, but not stable, expression of genes carried into cells by polyoma VP1 pseudocapsids. *Gene Ther*. **5,** 1410-1419
15. Braun, H., Boller, K., Löwer, J., Bertling, W.M. & Zimmer, A. (1999). Oligonucleotide and plasmid DNA packaging into polyoma VP1 virus-like particles expressed in *Escherichia coli. Biotechnol. Appl. Biochem*. **29,** 31-43
16. Sali, A. & Blundell, T.L. (1993) Comparative protein modeling by satisfaction of spatial restraints. *J. Mol. Biol*. **234,** 779-815
17. Yang, F., Moss, L.G. & Philips, G.N. (1996) The molecular structure of green fluorescent protein. *Nat. Biotechnol*. **14,** 1246-1251
18. Macias, M.J., Hyvönen, M., Baraldi, E., Schultz, J., Sudol, M., Saraste, M. & Oschkinat, H. (1996) Structure of a WW domain of a kinase-associated protein complex with a proline-rich peptide. *Nature (London)* **382,** 646-649
19. Kraulis, P. (1991) MOLSCRIPT: a program to produce both detailed and schematic plots of protein strutures. *J. Appl. Cryst*. **24,** 946-950
20. Merritt, E.A. & Bacon, D.J. (1997) RASTER 3D: photorealistic molecular graphics. *Methods Enzymol*. **277,** 505-524
21. Schmidt, U., Kenklies, J., Rudolph R. & Böhm, G. (1999) Site-specific fluorescence labelling of recombinant polyomavirus-like particles. *Biol. Chem*. **380,** 397-401
22. Böhm, G., Muhr, R. & Jaenicke, R. (1992) Quantitative analysis of protein far UV circular dichroism by neural networks. *Prot. Eng*. **5,** 191-195
23. Bork, P. & Sudol, M. (1994) The WW domain: a signalling site in dystrophin? *Trends Biochem. Sci*. **19,** 531-533
24. Sudol, M., Bork, P., Einbond, A., Kastury, K., Druck, T., Negrini, M., Huebner, K. & Lehman, D. (1995) Characterization of the mammalian YAP (Yes-associated protein) gene and its role in defining a novel protein module, the WW domain. *J. Biol. Chem*. **270,** 14733-14741
25. Koepf, E.K., Petrassi, H.M., Ratnaswamy, G., Sudol, M. & Kelly, J.W. (1999) Characterization of the structure and function of W $\rightarrow$ F WW domain variants: identification of a natively unfolded protein that folds upon ligand binding. *Biochemistry* **38,** 14338-14351
26. Chan, D.C., Bedford, M.T. & Leder, P. (1996) Formin binding proteins bear WWP/WW domains that bind proline-rich peptides and functionally resemble SH3 domains. *EMBO J*. **15,** 1045-1054
27. Koepf, E.K., Petrassi, M., Sudol, M. & Jeffrey, W.K. (1999) WW: an isolated three-stranded antiparallel β-sheet domain that unfolds and refolds reversibly: evidence for a structured hydrophobic cluster in urea and GdnHCl and a disordered thermal unfolded state. *Prot. Sci*. **8,** 841-853
28. Bedford, M.T., Chan, D.C. & Leder, P. (1997) FBP WW domains and the Abl SH3 domain bind a specific class of proline-rich ligands. *EMBO J*. **16,** 2376-2383
29. Macias, M.J., Gervais, V., Civera, C. & Oschkinat, H. (2000) Structural analysis of WW domains and design of a WW prototype. *Nat. Struct. Biol*. **7,** 375-379
30. Sahli, R., Freund, R., Dubensky, T., Garcea, R., Bronson, R. & Benjamin, T.L. (1993). Defect in entry and altered pathogenicity of a polyomavirus mutant blocked in VP2 myristylation. *Virology* **192,** 142-153
31. Scott, M. & Murad, K.L. (1998) Cellular camouflage: fooling the immune system with polymers. *Curr. Pharm. Des*. **4,** 423-438

Received November 14, 2000; revised March 16, 2001.

Fig. 1

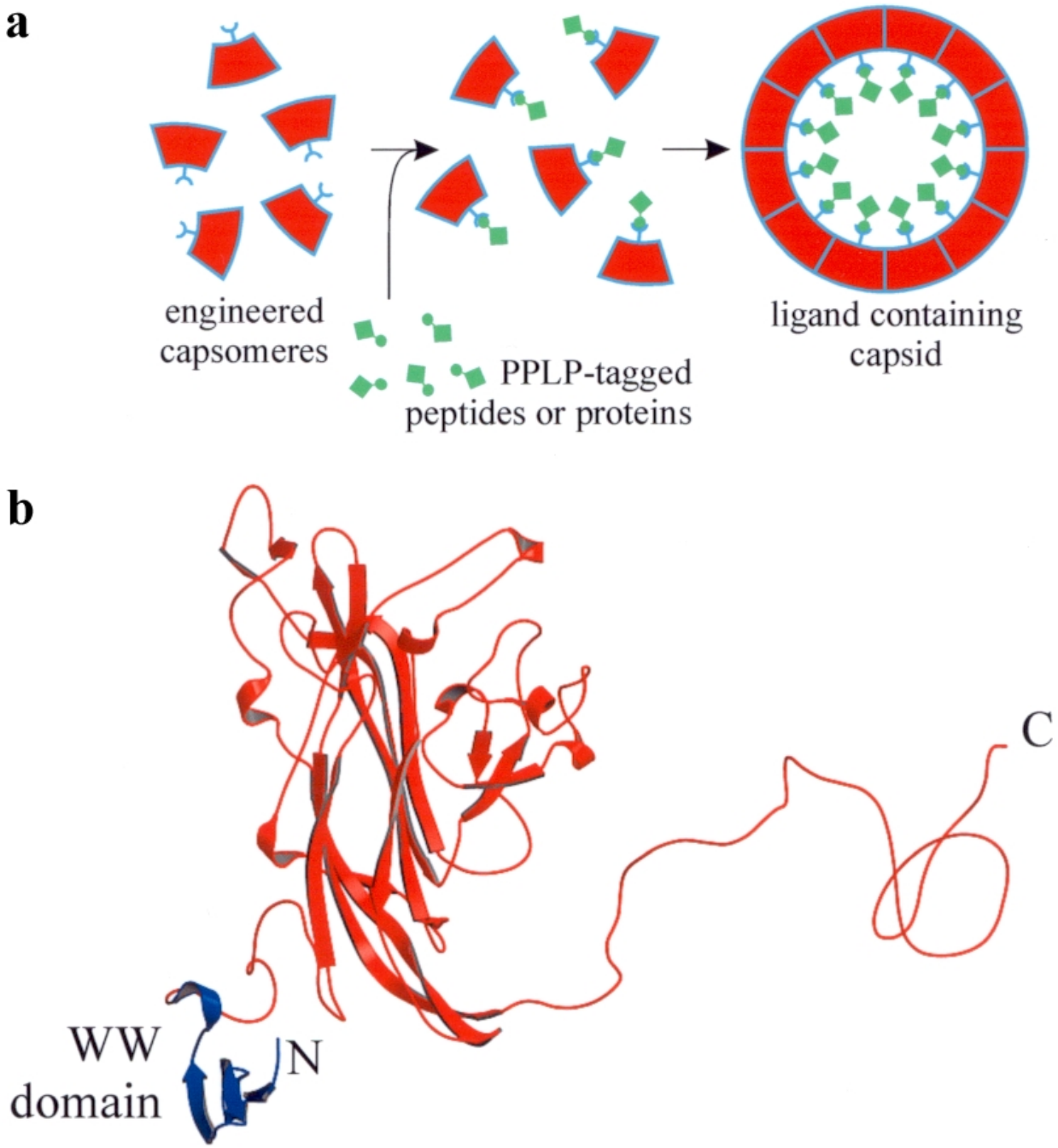

Figure 1. Principle of directed protein encapsidation. **(a)** The interaction of ligands with capsomeres is shown in a schematic representation of the in vitro assembly, leading to an encapsidation of the peptide or protein ligands into the particles. **(b)** To enable ligand-capsomere contacts, the interaction of WW domains with proline-rich sequences was utilized. The model shows the FBP11 WW domain fused to the N-terminal end of a VP1 monomer. The model is based on the reported X-ray structure of VP1 (9, 10) and the NMR structure of the YAP 65 WW domain (18).

Fig. 2

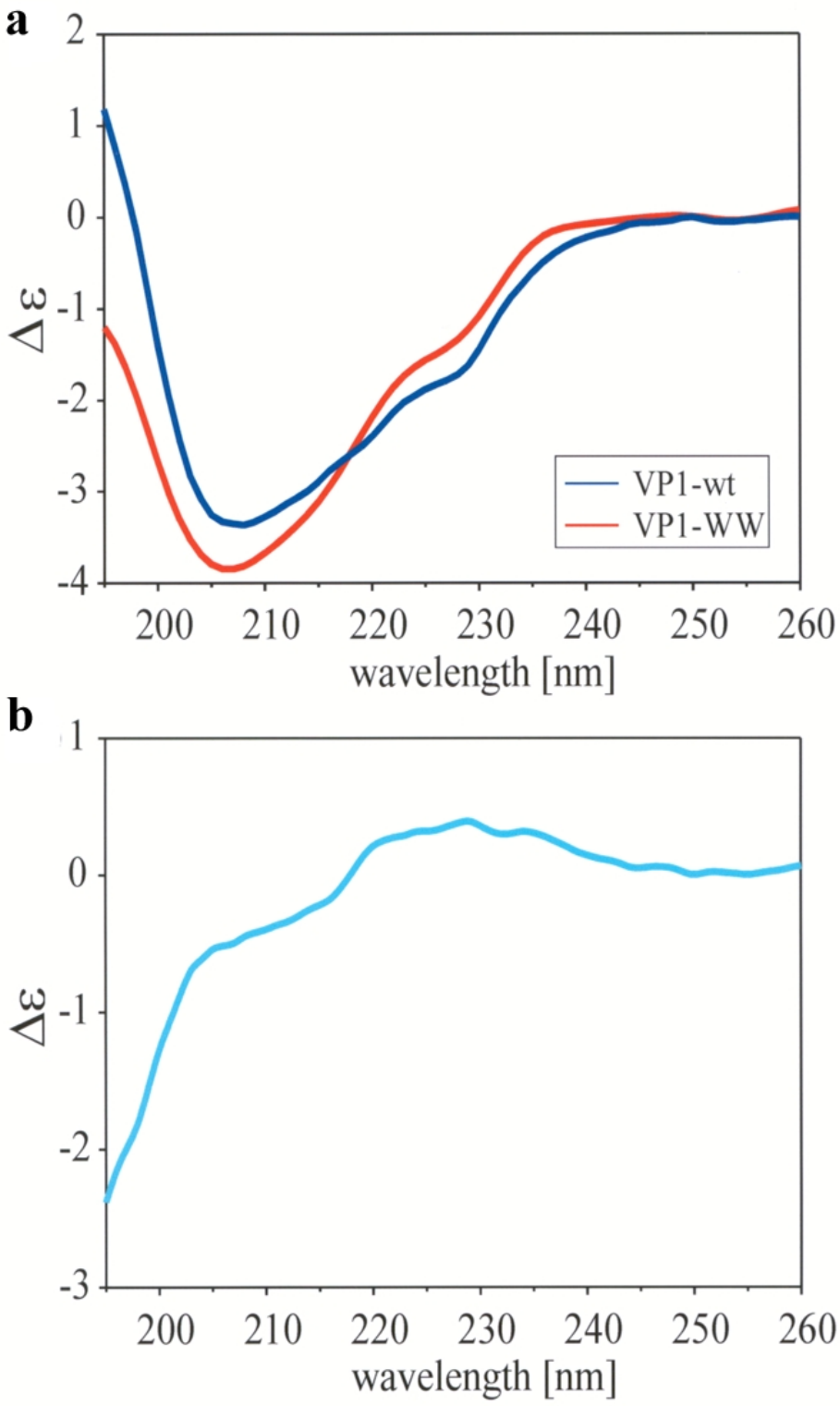

Figure 2. CD spectroscopy analysis of VP1-WW. **(a)** The far-UV CD spectrum of VP1-WW capsids differs significantly from the wild-type spectrum below 235 nm, indicating an altered secondary structure content caused by the three-stranded antiparallel β sheet of the WW domain (18) in the fusion protein. **(b)** The difference spectrum of VP1-WW minus wild-type VP1 closely resembles the spectrum of the isolated WW domain, which has the characteristic shape reported for WW domains (2).

Fig. 3

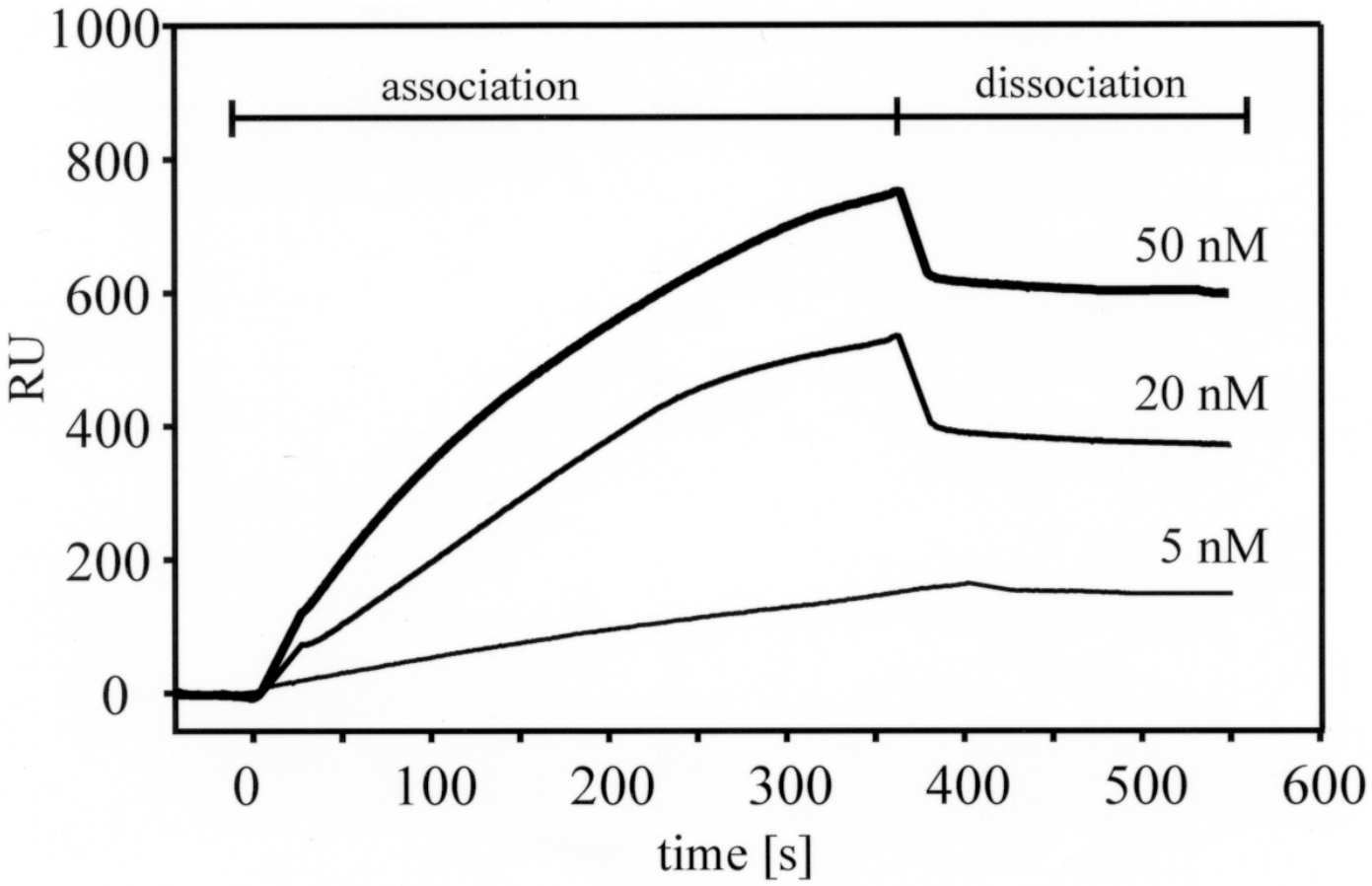

Figure 3. Surface plasmon resonance with immobilized PPLP peptide. Association and dissociation phases with different VP1-WW concentrations are shown. Simple Langmuir fits of the binding curves yielded an equilibrium dissociation constant $K_d = 40 \pm 5$ nM.

Fig. 4

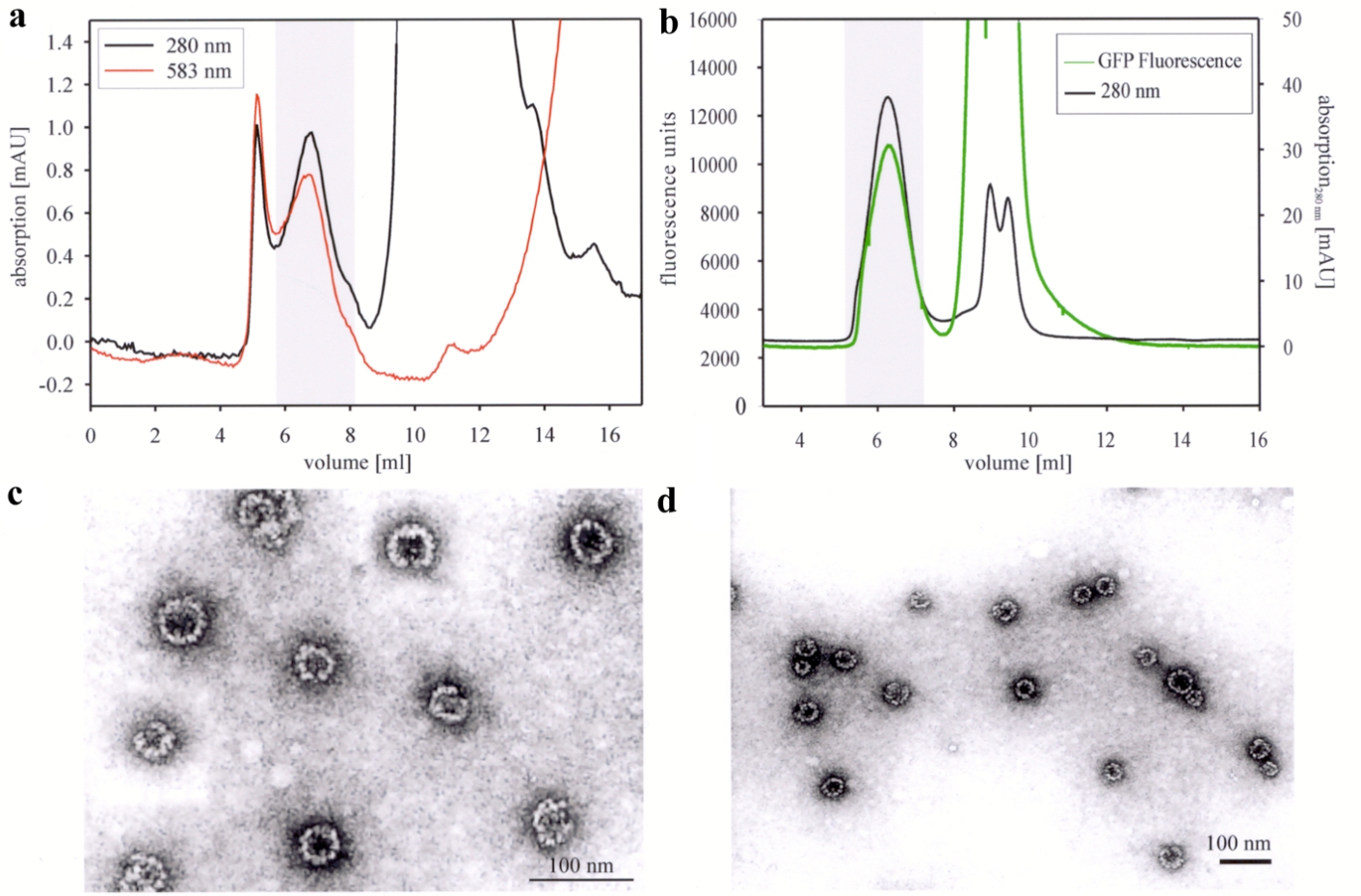

Figure 4. In vitro assembly and ligand encapsidation of VP1-WW. Size-exclusion chromatography profiles demonstrate that capsids contained the model ligands, either fluorescence-labeled PPLP peptide **(a)** or GFP **(c)**. For separation of the peptide-loaded capsids from unassembled pentamers and free peptide or GFP, two different columns were used (TSKgel 5000PW$_{XL}$ for the peptide-loaded capsids, TSKgel 6000PW$_{XL}$ for the GFP-containing capsids). The fractions that were collected for further experiments are highlighted in gray. Electron micrographs revealed a homogeneous population of PPLP-peptide-containing particles **(b)** and GFP-containing capsids **(d)**, which were both morphologically indistinguishable from wild-type capsids.

Fig. 5

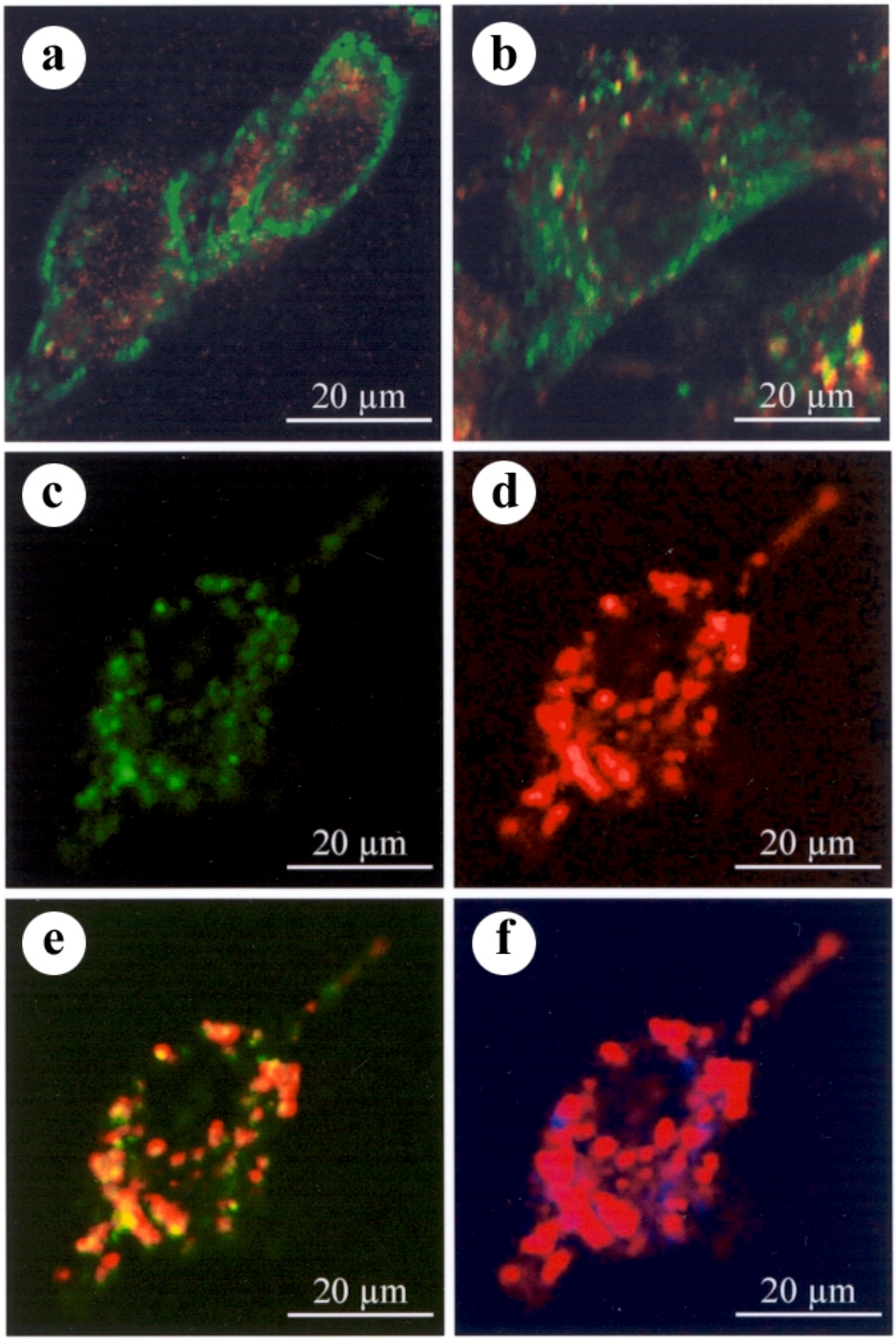

Figure 5. Delivery of fluorescence-labeled PPLP peptide into NIH 3T3 cells by fluorescein-labeled PPLP-peptide-containing virus-like particles. **(a)** After 30 min of incubation, the peptide-containing particles first appeared in endocytotic vesicles close to the cell membrane and the peripheral cytoplasm. **(b)** During further incubation (total of 2 h), the particles either migrated into the cytoplasm or were degraded in lysosomes; the latter case is indicated by yellow (colocalization of lysosomes, red; encapsidated ligands, green). **(c-f)** To determine whether encapsidated ligands can be released intracellularly from the capsids, capsomere proteins (green, *c*), ligands (red, *d*), and lysosomes (blue, *e*) were used simultaneously in a single experiment. Superposition of the capsomere images and ligand images showed a partial release of the ligands from the capsids (*e*). Superposition of ligand and lysosome images confirmed partial targeting of the ligands to lysosomes (*f*).